Korean Journal of Radiology

KJR

Check for updates

Pearls and Potential Pitfalls for Correct Diagnosis of Ovarian Cystadenofibroma in MRI: A Pictorial Essay

Giacomo Avesani[1], Gianluca Caliolo[1], Benedetta Gui[1], Federica Petta[1], Camilla Panico[1], Viviana La Manna[2], Francesca Moro[2], Antonia Carla Testa[2, 3], Giovanni Scambia[2, 3], Riccardo Manfredi[1, 4]

[1]Dipartimento di Diagnostica per Immagini, Radioterapia Oncologica ed Ematologia, Fondazione Policlinico Universitario A. Gemelli IRCCS, Rome, Italy; [2]Dipartimento Scienze della Salute della Donna, del Bambino e di Sanità Pubblica, Fondazione Policlinico Universitario A. Gemelli, IRCCS, Rome, Italy; Departments of [3]Obstetrics and Gynecology and [4]Radiology, Catholic University of the Sacred Heart, Rome, Italy

Ovarian cystadenofibroma is a benign ovarian tumor that is characterized by a consistent percentage of masses, which remain indeterminate in ultrasonography and require magnetic resonance (MR) investigation; they may mimic borderline or malignant lesions. Three main morphologic patterns, resembling different ovarian neoplasms, can be identified in cystadenofibromas: multilocular solid lesions, unilocular cystic lesions with parietal thickening, and purely cystic masses. However, a cystoadenofibroma has typical features, such as T2-weighted hypointensity associated with no restrictions in diffusion-weighted imaging (the so-called "dark-dark appearance") and progressive post-contrast enhancement (type I perfusion curve). The purpose of this study was to review the features of ovarian cystadenofibromas in MR imaging and to suggest pearls and pitfalls regarding their correct diagnosis.
Keywords: *Cystadenofibroma; MR imaging; Ovarian neoplasm; Epithelial-stromal tumours*

INTRODUCTION

Ovarian cystadenofibromas are uncommon ovarian tumors that contain dense fibrous stroma, in combination with epithelial cystic components. These tumors are classified according to epithelial cell types: serous, endometrioid, mucinous, clear-cell, and mixed; the serous type is the most common type (75%) [1,2]. The degree of epithelial proliferation is used for the classification of benign, borderline, and malignant tumors, although malignant

cystadenofibroma is extremely rare [3,4]. In most cases, this tumor involves a single ovary and rarely affects both ovaries.

Most cystadenofibromas show no signs or symptoms and are discovered incidentally during routine gynecological ultrasound performed for other reasons. When present, symptoms include lower abdominal pain or discomfort, vaginal bleeding, and a palpable mass in the abdomen [1,4-6]. The appearance of cystadenofibromas in imaging may often be misleading, as their typical appearance is a multilocular cystic mass with a solid nodular component [3,7,8].

With the use of preoperative imaging modalities, including ultrasonography (US), computed tomography (CT), and magnetic resonance (MR) imaging, these tumors may be diagnosed as malignant lesions due to their solid components or thick septa. The tumor may also have the typical appearance of an ovarian malignancy, even at the time of surgery. However, some imaging features can aid in differentiating benign tumors from others, potentially providing accurate preoperative diagnosis, and could help in avoiding

unnecessary extensive surgical interventions.

In our recent experience at a referral center for ovarian cancer, we analyzed 46 ovarian masses, which were inconclusive upon US using the "International Ovarian Tumor Analysis (IOTA) simple rules" classification [9]; of these, 16 were cystadenofibromas and, among them, 5 were misdiagnosed as borderline tumors. This demonstrates the importance of radiologists in identifying this rare ovarian tumor with certainty and knowing its peculiar characteristics to correctly suggest the best treatment for patients. In this article, we review the features of ovarian cystadenofibromas in MR imaging in order to suggest pearls and pitfalls for their correct diagnosis and to provide a wide collection of images.

Table 1. Pelvis MRI Protocol to Characterize Adnexal Masses and Scanning Parameters

Parameter	1.5T					
	Sagittal T2WI	Axial T2WI HR	Axial GRE 3DT1WI (Dixon)	Axial DWI	Axial DCE (PWI) T1WI	Axial GRE 3DT1WI (Dixon)
TR, ms	5891	11000	7.6	14879	3.1	7.6
TE, ms	80.5	74.1	Minimum	Minimum	Minimum	Minimum
Echo train length	24	23	23	-	-	23
Flip angle, °	160	160	15	-	20	15
FOV, cm	24	30	30	30	30	30
Matrix size	288 x 288	352 x 224	320 x 224	128 x 128	256 x 224	320 x 224
Slice thickness, mm	4	5	6	5	3	6
Slice interval, mm	0.4	1.0	-	1.0	-	-
b-value, s/mm^2	-	-	-	1000	-	-
Acquisition time, s	2:51	4:57	0:27	5:21	5:02	0:27

DCE = dynamic contrast enhanced, DWI = diffusion-weighted imaging, FOV = field of View, GRE = gradient echo sequense, HR = high resolution, PWI = perfusion weighted imaging, TE = echo time, TR = repetition time, T1WI = T1-weighted image, T2WI = T2-weighted image, 3D = three-dimensional
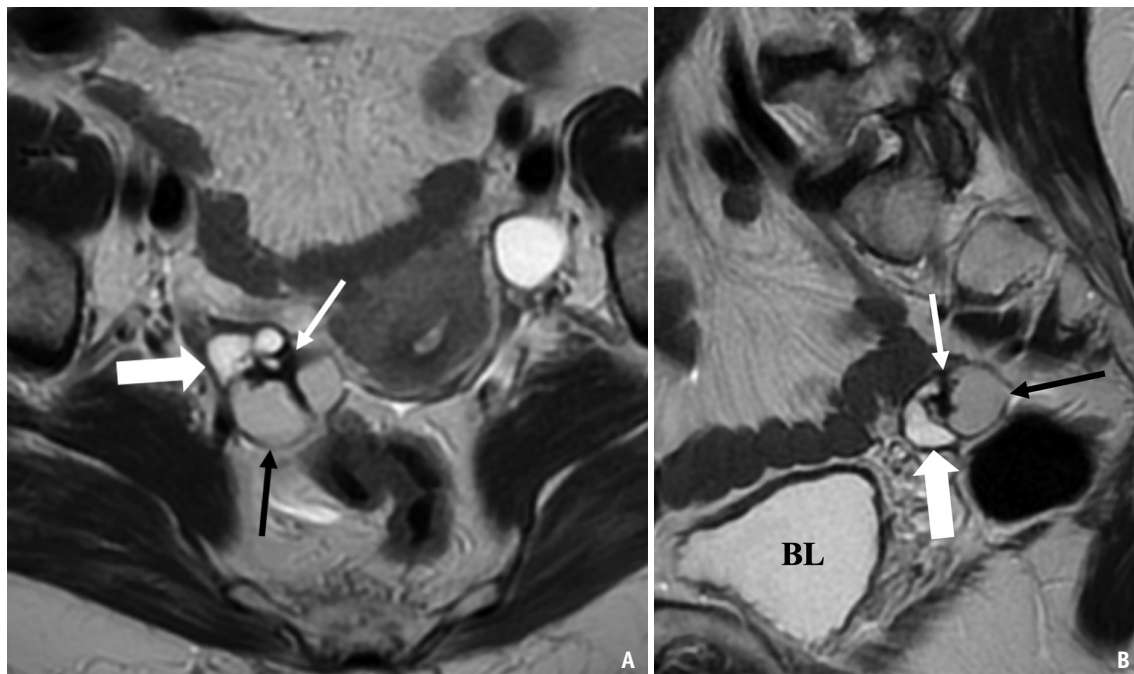
Fig. 1. A 77-year-old female with right, pathologically proven, mucinous ovarian cystadenofibroma (type I: multilocular solid lesion).
A, B. Axial **(A)** and sagittal **(B)** T2-weighted MR images depict a multilocular lesion with variable signal intensities among the loculi (thick white arrows: higher serous signal intensity; black arrows: lower signal intensity owing to the high protein content and viscosity) and a solid fibrous area (thin white arrows) between the smoothly thickened septa. Note that the solid component shows a very low-T2 signal intensity, similar to skeletal muscle. BL = bladder

Imaging Evaluation

US is the first imaging modality used to investigate ovarian masses and can correctly diagnose 80%–85% of cases [10-12]. Diagnostic tools, such as the "IOTA simple rules", have been designed to discriminate between benign and malignant ovarian masses.

In US, ovarian cystadenofibromas commonly appear as unilocular solid cysts with one or more papillary projections, followed by a multilocular solid mass with a small solid component pattern. Most cystadenofibromas have solid components; papillary projections were described in half of them, mostly without significant color Doppler signals [13].

However, 15%–20% of all ovarian masses remain unspecified after US. In such cases, MRI is the modality of choice to further investigate the nature of the mass [3,4,7]. CT of the thorax and abdomen is usually limited to staging of the disease in cases of suspected malignant masses [14]. Table 1 shows the MRI protocol used to investigate indeterminate ovarian masses in our center.

MR Imaging Characteristics

Since cystadenofibromas are benign, adnexal neoplasms composed of fibrous tissue, they demonstrate a very low-signal-intensity appearance in T2-weighted MR images, which results from the T2-shortening effects of collagen. Typically, multiple cystic locules filled with fluid show homogeneous, high signal intensity in T2-weighted images; the appearance of the individual locules may also vary due to differences in the degree of hemorrhage or protein content (e.g., mucinous differentiation) (Fig. 1). In T1-weighted images, the masses show low to intermediate signal intensities, equal to or slightly below that of the myometrium. In diffusion-weighted imaging (DWI), the fibrous tissue does not show any restriction and is typically hypointense on high-b-value imaging (Fig. 2) [15].

After administration of gadolinium, the solid parts showed mild enhancement. Using a semi-quantitative analysis, the curve initially shows an enhancement lower than that of the myometrium, followed by a slow and progressive increase in the later phases [16] (type I curve, following the O-RADS classification [17]) (Fig. 3). The imaging appearance of cystadenofibromas varies depending on whether cystic or fibrous components predominate. Three broad morphological patterns have been identified on MR imaging [3,7,15,16,18].
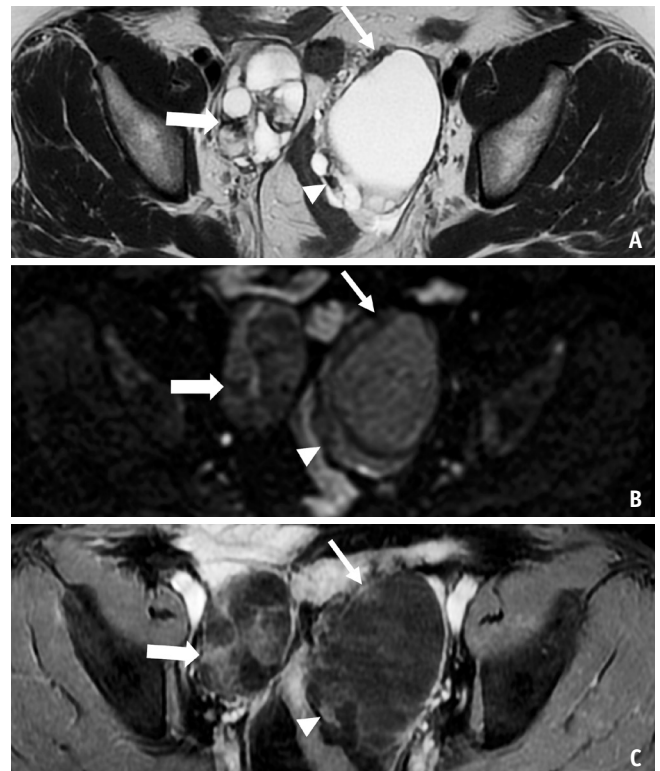
Fig. 2. A 47-year-old female with bilateral ovarian serous cystadenofibroma (type I: multilocular solid lesion).
A. The T2-weighted, spin-echo image in the axial plane shows a predominantly cystic mass of the left ovary with fibrotic low-signal intensity, irregular thickness of the wall (thin arrow), a mural nodule (arrowhead), and a smaller multilocular mass arising from the right ovary; note that the solid component and thick septa (thick arrow) in the right mass have a lower signal intensity on the T2-weighted image than the ovarian stroma. **B.** The high b-value (b =1000), diffusion-weighted image demonstrates a hypointensity of the stromal components described above (thin and thick arrows, arrowhead). **C.** Axial, post-contrast, T1- weighted image showing slight enhancement of the irregular thickness of the wall (thin arrow), mural nodule (arrowhead), and septa (thick arrow).

Type I, Multilocular Solid Lesion: Multilocular Complex Cystic Mass with Solid Nodular Component ("Black Sponge"-Like Appearance)

Type I lesions are the most frequent MRI appearance, consisting of a multiseptated, predominantly cystic mass with variable amounts of solid nodular components. They are seen as well-defined, nodular, solid areas protruding into the cystic locules of the tumors. They typically demonstrate a very low signal intensity, similar to that of the skeletal muscle in T2-weighted imaging. The solid component within the mass reflects dense fibrous stromal proliferation and contains multiple, small, inner cystic, glandular structures that are either round or ovoid. They typically show mild enhancement after administration of
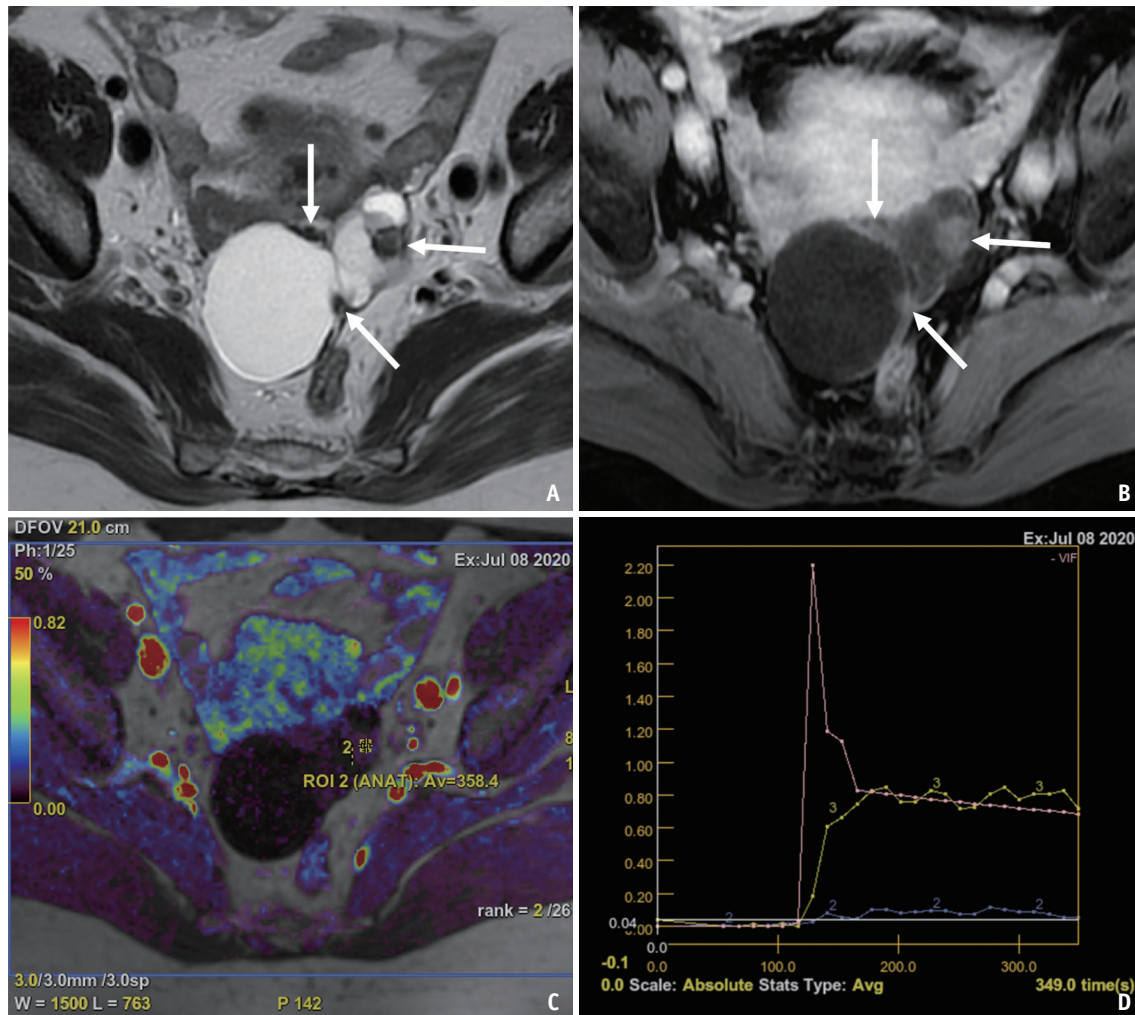
Fig. 3. A 58-year-old female with pathologically proven benign serous cystadenofibroma of the ovary (type I: multilocular solid lesion).
A. The T2-weighted, axial image shows a multilocular cystic mass with solid components in the left ovary. The solid component (arrows) demonstrates low-T2 signal intensity (similar to skeletal muscle). The serous cystic portions of the tumor show homogeneous high signal intensity on the T2-weighted images. **B.** The contrast-enhanced, T1-weighted, axial image with fat-suppression shows mild enhancement in the solid components within the mass (arrows). **C, D.** Color map shows areas of maximum enhancement. An region-of-interest is placed within the enhancing solid nodule on the left. In the perfusion study, this nodular area (curve number 2) presents a low and only slightly increasing post-contrast enhancement (type I curve); curve number 3 represents the enhancement of the myometrium.

intravenous, gadolinium-based contrast media.

The margins of the solid component of ovarian cystadenofibroma are smooth and have a well-defined outline, in contrast to ovarian malignancy. The MR appearance of the cystic components is non-specific and usually consists of numerous cystic loculations. This is in contrast to most benign serous cystadenomas, which are usually unilocular or bilocular. The cystic component usually has a smooth contour, thin regular septa, and no endocystic papillary projections (Fig. 4). This black, sponge-like appearance [18,19] corresponds to tiny, scattered, fluid-filled cavities with a higher signal intensity within the dark-signal-intensity

solid component in T2-weighted images. This appearance has to be considered a characteristic of cystadenofibroma, but these findings may not be evident in all cases.

Type II, Bilocular or Unilocular Cystic Mass with Plaque-Like Thickenings ("Carpet Like" Pattern)

Type II lesions are predominantly cystic, with diffusely or partially thickened walls with dark signal intensity in T2-weighted sequences. The lesion exhibited varying degrees of wall thickness (possibly > 3 mm) associated with a plaque-like appearance, or focal pseudo-nodular thickening, that is enhanced following the administration of intravenous,
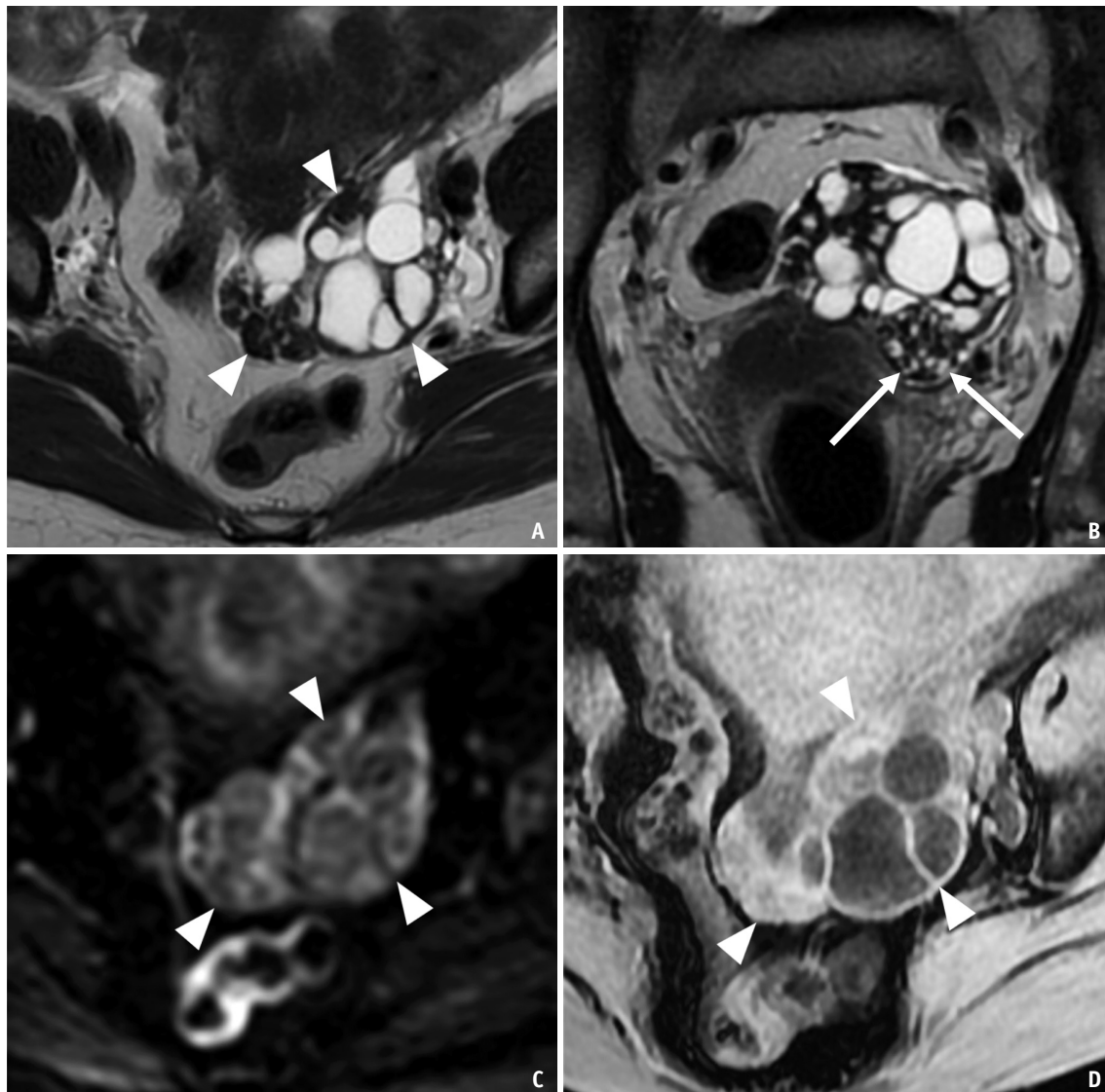
Fig. 4. A 51-year-old female with left ovarian cystadenofibroma (type I: multilocular solid lesion).
A. The T2-weighted, axial image shows a complex mass with a lobular contour, multiple cysts, and fibrotic solid components. Because of their collagen content, both nodular solid areas and thick septa (arrowheads) demonstrate a very low-T2 signal intensity. **B.** T2-weighted, coronal images of the same mass; note the presence of multiple, tiny, cystic changes within the solid portion (arrows). **C.** The diffusion-weighted image (b = 1000) demonstrates hypointensity of the stromal components (arrowheads) with no diffusion-restricted areas. **D.** Axial, gadolinium-enhanced, T1-weighted, fat-saturated, MR image shows enhancement with mild signal intensity of the solid components and thick septa (arrowheads).

gadolinium-based contrast medium. This dark-signal-intensity thickening represents a dense fibrous component within the wall (Fig. 5).

Type III, Purely Cystic Mass Resembling Serous Tumours

The type III pattern is very similar to that of serous ovarian cystadenoma on MRI. Small foci of fibrous stomas were detected, and the lesion manifested as a unilocular or multilocular mass with entirely cystic components and absent solid tissue structures (Figs. 6, 7).

Cystadenofibromas differ from serous cystadenomas, as the connective tissue component in cystadenomas is a minor and merely supportive element, while cysts are a major feature.

In our experience, type I was the most common pattern, followed by types II and III. Of the histologically proven 16 cystadenofibromas undiagnosed at US analysed in 2020, 10 were type I, four were type II, and two were type III. A co-existing uterine, tubal, and contralateral ovarian pathology is often observed, which usually has no significance in the
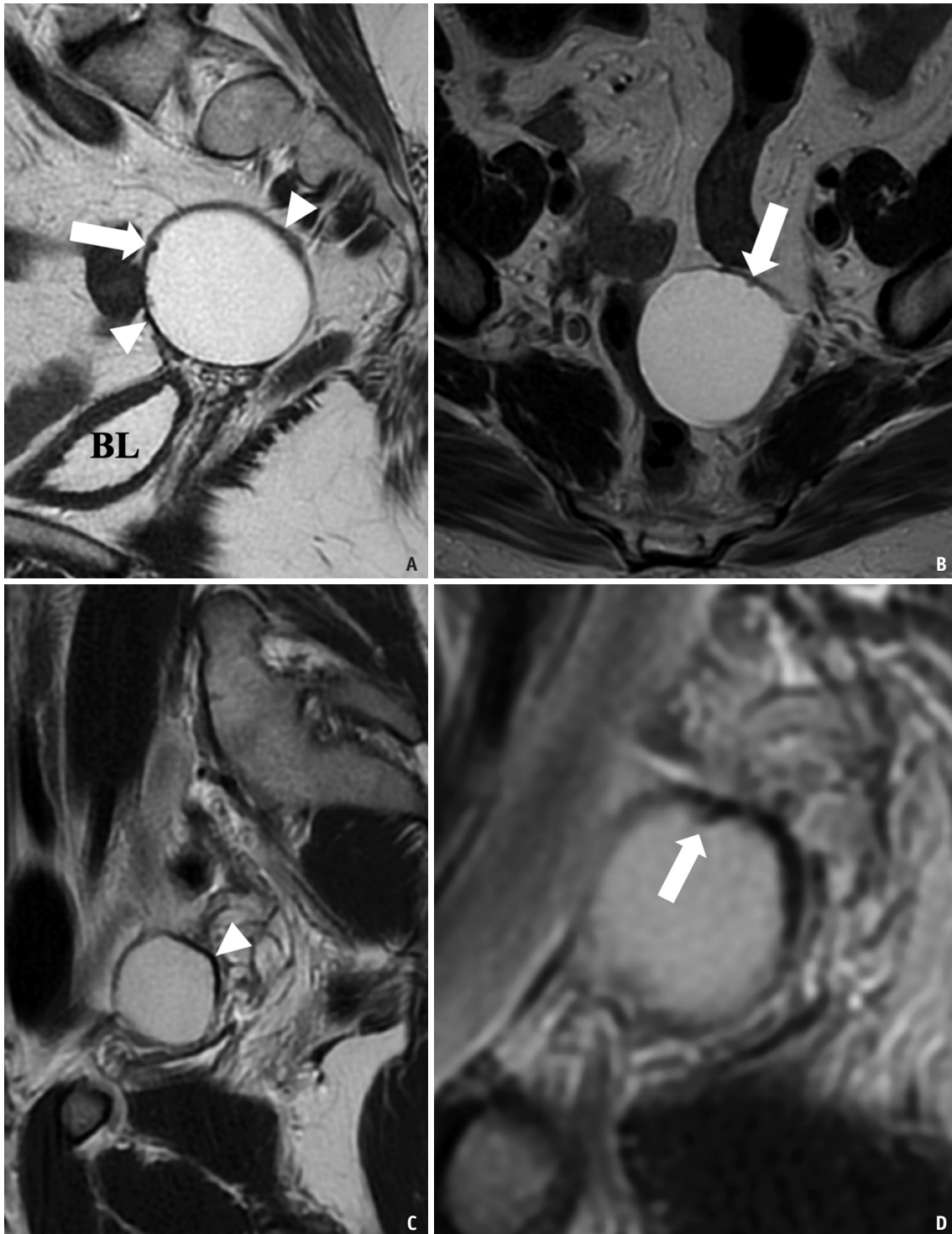
Fig. 5. Two examples of serous cystadenofibroma of two different patients [42-year-old (A, B) and 36-year-old female (C, D)]; type II: unilocular cystic mass with plaque-like thickenings.
A, B. Sagittal **(A)** and axial **(B)**, T2-weighted images show a large cystic mass with diffusely thickened, low-intensity walls (arrowheads) with associated focal pseudo-nodular thickening arising from the anterosuperior surface of the mass (arrows). Dark-signal-intensity thickening represents a dense fibrous component within the wall. **C, D.** Sagittal, T2-weighted image another example of a unilocular serous cystadenofibroma **(C)** surrounded by a partly thickened wall of dark signal intensity (arrowhead) in the left ovary. In another slice of the same lesion **(D)**, a hypointense sessile tissue arising from the posterior wall of the mass is visible (arrow). BL = bladder
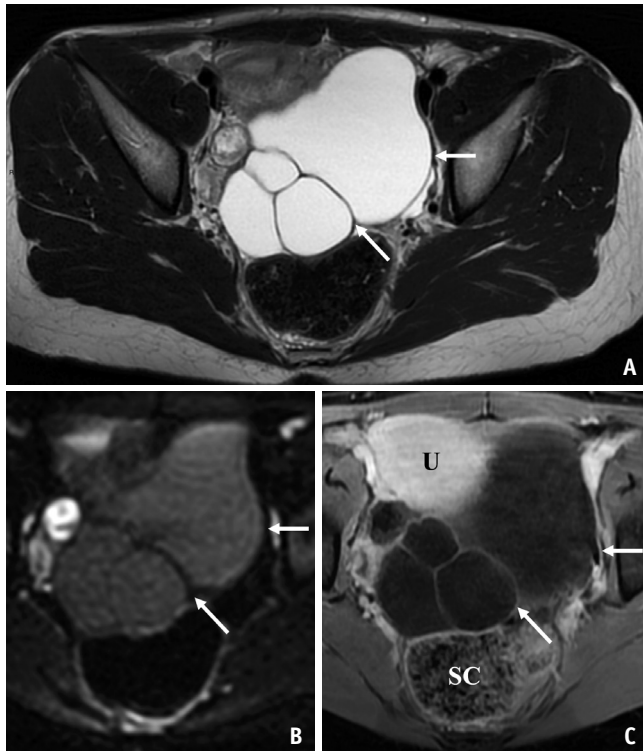
Fig. 6. A 23-year-old female patient with a multilocular cystadenofibroma of the left ovary (type III: purely cystic mass).
A. T2-weighted, axial, MR image demonstrates a large multilocular mass with entirely cystic elements and the absence of a gross solid tissue structure, mimicking a serous cystadenoma. Note the homogeneous MR signal intensity of the different locules, thick regular septa, and no endocystic or exocystic vegetation. There is evidence of dark-signal intensity tissues which lie within the wall and septa (arrows); a finding that is specific for a stomal tissue. **B.** Diffusion-weighted image (b = 1000) demonstrates hypo-intensity of the connective component (arrows). **C.** Axial, gadolinium-enhanced, T1-weighted, fat-saturated, MR image shows relative enhancement with mild signal intensity of the wall and septa (arrows). SC = sigmoid colon, U = uterus

development of ovarian cystadenofibromas. There is no evidence of endocrine activity in ovarian cystadenofibroma; therefore, imaging studies should not show any association with uterine enlargement, endometrial thickening, or polyps [4,20]. Lymphatic involvement or ascites has never been reported [7].

Differential Diagnosis

Classically, cystadenofibromas are differentially diagnosed with other ovarian masses that have similar low-T2 signals, mainly due to the fibrous component [19,21]. Additionally, T2-hypointense ovarian lesions are fibromas [3,14,22], Brenner tumors [23], struma ovarii

[24], metastatic ovarian tumors with a highly fibrous component, particularly those from the gastrointestinal tract [25], and endometriomas.

Fibromas are ovarian masses composed of fibrous tissue; they usually have no cystic component, even if cystic degeneration is possible; when cystic degeneration is present, it tends to be central and has a more irregular interface with solid tissue than in cystadenofibromas. Moreover, the tissue near the cystic components is usually more hyperintense than muscle on T2-weighted images [26]. Brenner tumors are usually predominantly solid and may have coarse calcifications, which are rare in cystadenofibromas. Struma ovarii may be a multiocular solid mass with T2-hypointense components. If it coexists with a mature teratoma, the presence of a fat component excludes the diagnosis of cystadenofibroma. If a fat component is not present, the cystic components usually have different signal intensities; the more important considerations for differential diagnosis are those containing colloid, which may either be hypointense in both T1- and T2-weighted images or hyperintense in fat-suppressed, T1-weighted images [24], with no internal enhancement (Fig. 8). Endometriomas are usually easily differentiated because of their characteristic blood components, which are not present in cystadenofibroma. Metastatic ovarian tumors with fibrous components are usually larger than cystadenofibromas. They also have solid components that are strongly enhanced and slightly hyperintense in T2-weighted images.

In our experience, challenges arise in the differential diagnoses of epithelial neoplasms, especially with serous borderline tumors, particularly for unilocular or bilocular cysts with irregular walls. The classically described features for the prediction of ovarian malignancy are as follows: a lesion size of > 4 cm, thickness of the walls and septa exceeding 3 mm, internal structure including papillary projections, nodularity, variable degrees of the solid components, necrosis, hemorrhage, and a heterogeneous and early enhancement pattern. Thus, according to these criteria, the imaging findings of cystadenofibroma may be misinterpreted as a malignant mass [19].

Most cystadenofibromas have some US-associated characteristics [13] that may support a correct diagnosis, but many of them have features that mimic borderline tumors, necessitating MR imaging as second-level imaging. In 2020, 70% of cystadenofibromas examined with MR imaging were multilocular; in US, unilocular patterns
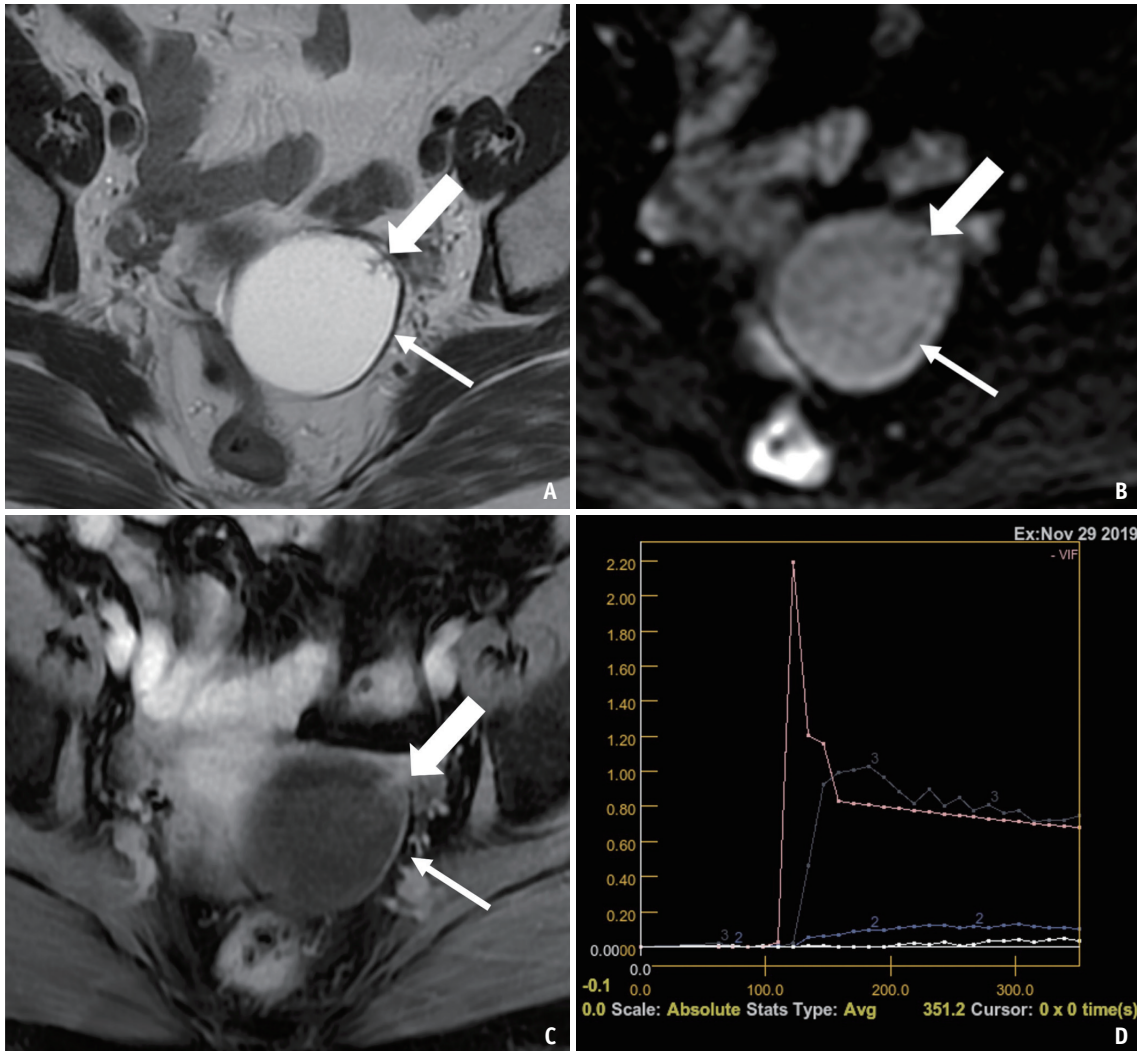
Fig. 7. A 56-year-old female with pathologically proven cystoadenofibroma of the left ovary with lower abdominal pain (type II: unilocular cystic mass with plaque-like thickenings).
A. An axial, T2-weighted, spin-echo image shows a well-defined, homogeneous, cystic mass with partially thickened, dark-signal-intensity walls (thin arrow) and a solitary papillary projection (thick arrow) with low signal intensity. **B.** The lesion shows low signal intensity (thin and thick arrows) on diffusion-weighted imaging with a b-factor of 1000 (no restriction). **C.** Fat-suppressed, T1-weighted, gradient-echo, MR image obtained after the administration of gadopentetate dimeglumine demonstrates enhancement of the papillary projection (thick arrow) and of the thickened wall (thin arrow). **D.** MR perfusion showed a slow rising enhancement type I curve of the papillary projection (curve labelled as 2; the curve labelled as 3 is the one of the myometrium). The final histopathological diagnosis was left ovarian serous cystadenofibroma.

showed solid components. Additionally, multiple papillary projections were observed in 80% of US cases. The main confounding characteristics include the presence of a mildly enhanced, solid component, a thick, irregular septa, or a walled, cystic mass.

However, two important findings suggestive of a correct diagnosis should be identified:

1) The "dark-dark appearance" of the solid component: as mentioned, the main characteristic of cystadenofibromas is a dense fibrous tissue contained in the solid component of the tumor. This tissue is hypointense on T2-weighted

imaging because of collagen (the first "dark"). The fibrous tissue does not show restriction in DWI; therefore, it is visualized as hypointense in both low and high b-value images (the "second dark"). This may correspond to the hypointensity of the fibrous tissue in the apparent diffusion coefficient maps. Papillary projections and mural nodules of borderline ovarian tumors are usually less hypointense than fibrous tissues (when not slightly hyperintense). Furthermore, even if they are hypointense on T2-weighted imaging, they show mild to strong restriction on DWI (Fig. 7).

2) Type I curve of enhancement: fibrous tissue, like
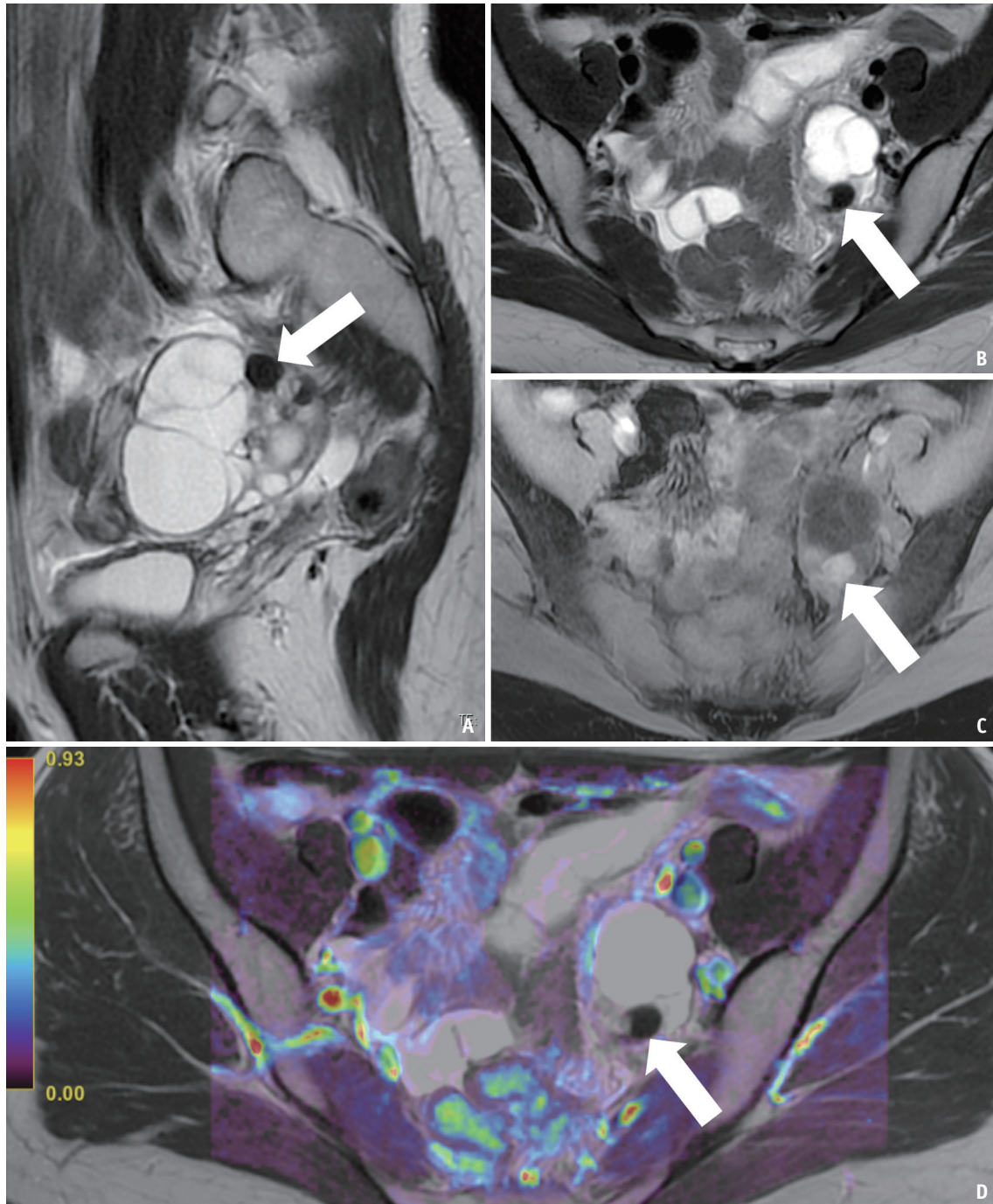
Fig. 8. A 29-year-old female with a struma ovarii of the left ovary.
A. Sagittal, T2-weighted image shows a multilocular mass with varying intensities of the cystic components. In particular, a hypointense component (arrow) is visible in the upper part of the lesion. **B, C.** Axial, T2-weighted image **(B)** of the same T2-hypointense component (arrows) of the lesion, which is hyperintense in T1-weighted image with fat saturation **(C)**. **D.** In the fused T2-weighted and perfusion image, no enhancement is visible. This component (arrow) is consistent with colloid.

in other parts of the body, has poor vascularization. As such, enhancement is typically mild and progressive. Our MR imaging protocol for indeterminate ovarian masses includes a perfusion study during contrast injection; all cystadenofibromas show a type I curve. Borderline and malignant lesions usually show type II or III curves, characterized by a steep increase in intensity in the first part of the curve, followed by a slight decrease in later
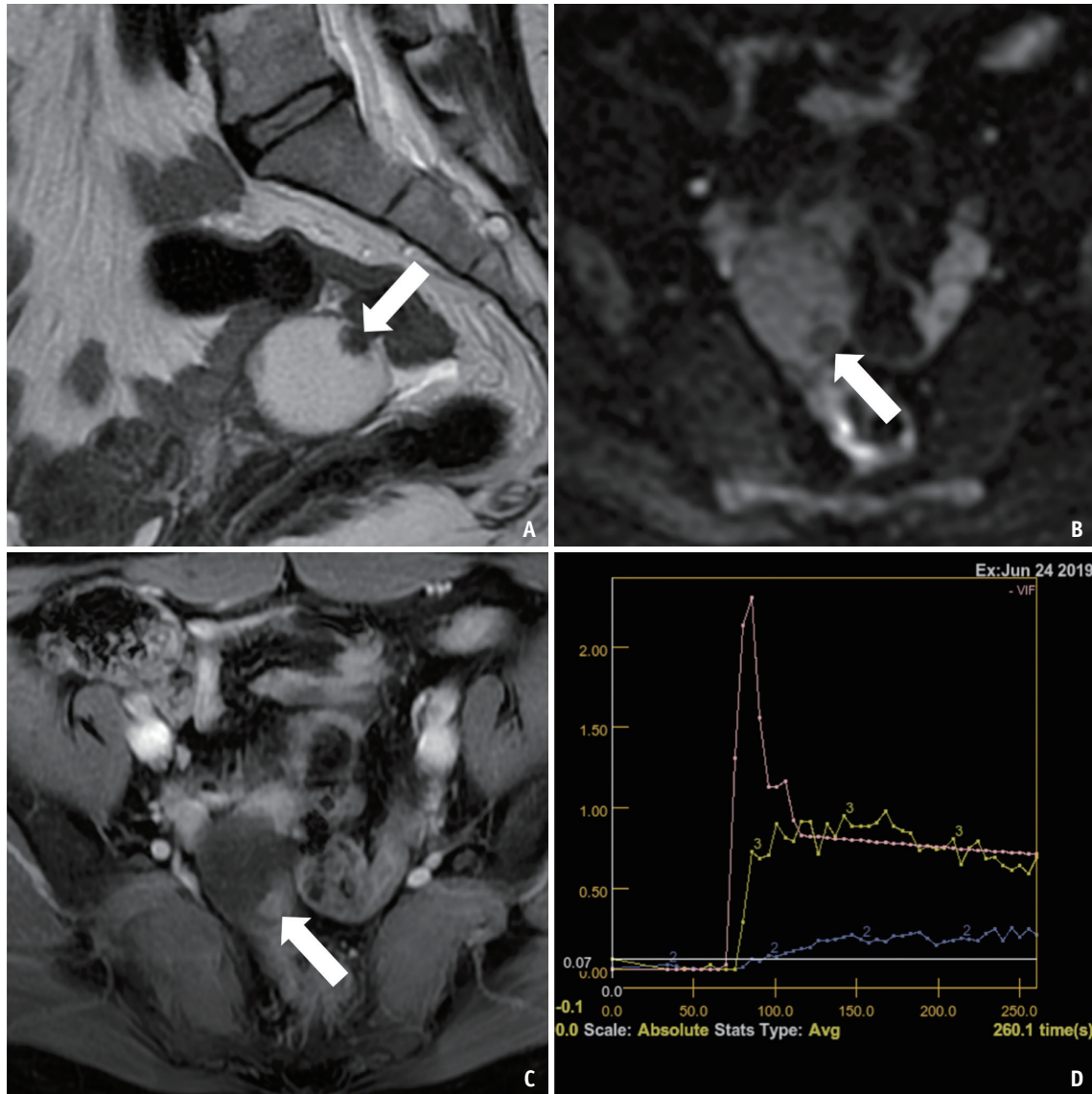
Fig. 9. A 52-year-old female with serous cystadenofibroma of the right ovary (type I: unilocular solid lesion).
A. Sagittal, T2-weighted, fast spin-echo image shows a well-defined, unilocular, solid mass with partially thickened, dark-signal-intensity walls and a hypointense mural nodule arising from posterior surface (arrow). **B.** Axial diffusion-weighted imaging (b = 1000) of the same lesion in **(A)**: the mural nodule (arrow) shows low signal (no restriction). **C, D.** Fat-suppressed, T1-weighted, gradient-echo, MR image obtained after the administration of gadopentetate dimeglumine demonstrates enhancement of the mural nodule (arrow) **(C)**; an region-of-interest located in the mural nodule shows its slightly increasing enhancement (type I curve; curve number 2 in the figure) during the perfusion study (curve number 3 is that of myometrium) **(D)**.

phases (Figs. 9, 10).

CONCLUSION

Ovarian cystadenofibromas may have different presentation patterns, some of which may be misleading because of their similarities with borderline and malignant lesions, particularly multilocular solids. Knowing the main presentation patterns described in this article is important for radiologists to reach a correct diagnosis. The two most important MR features, which help to correctly diagnose cystadenofibroma, are the "dark-dark" appearance of solid tissue and the slow, continuous increase of the enhancing curve measured during perfusion (type I curve).

Conflicts of Interest
The authors have no potential conflicts of interest to disclose.
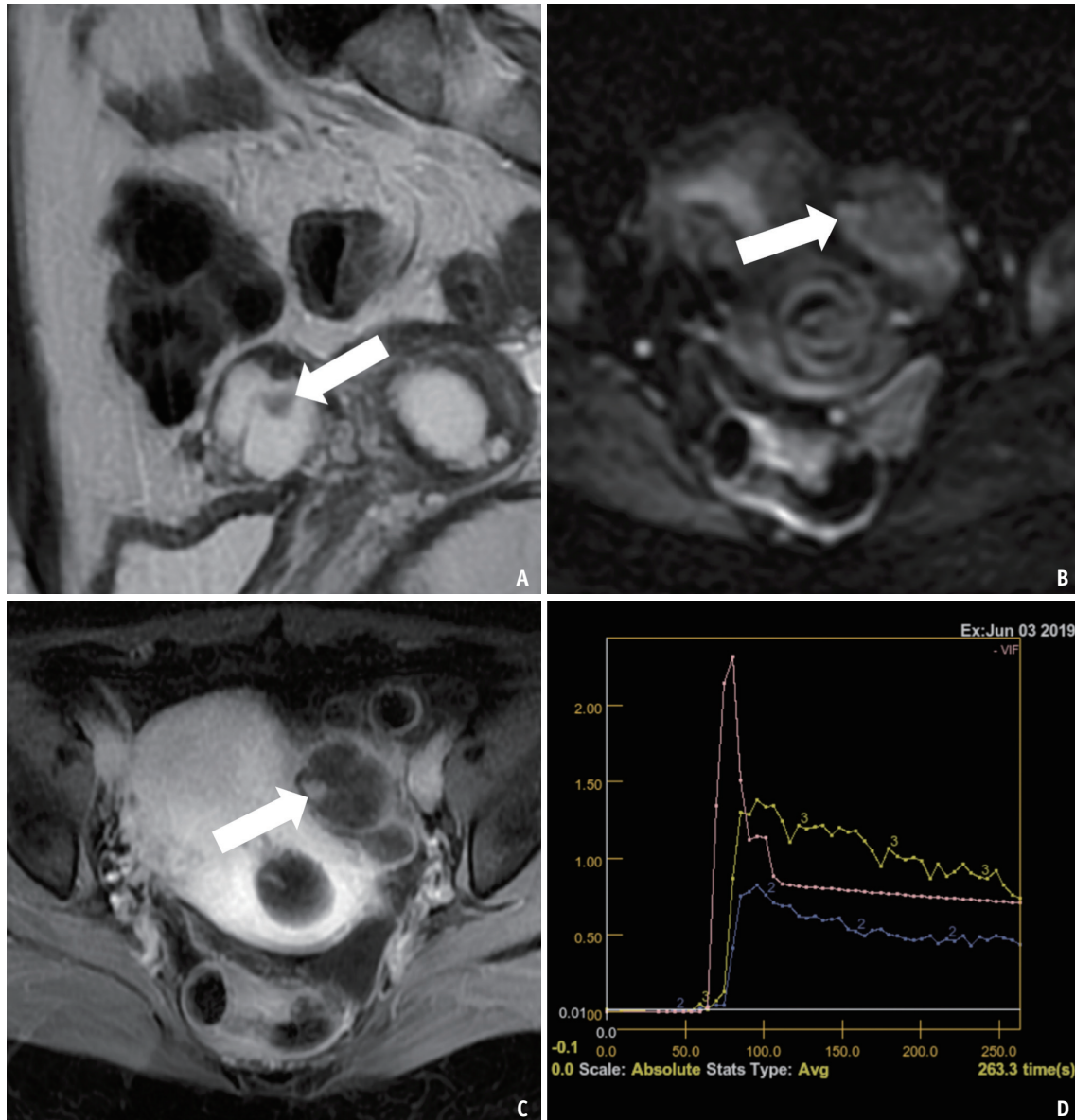
Fig. 10. A 41-year-old female with a borderline cystadenoma of the left ovary.
A. The sagittal T2-weighted image revealed a bilocular-solid adnexal lesion of the left ovary with thin septation and a posterior mural nodule (arrow). **B.** Axial DWI (b = 1000) of the same lesion: the nodular lesion (arrow) shows high signal intensity in high b-value DWI (which corresponds to a hypointensity in the apparent diffusion coefficient map -not shown-), consisting in a restricted diffusion. **C.** Fat-suppressed, T1-weighted, gradient-echo, MR image obtained after the administration of gadopentetate dimeglumine demonstrates enhancement of the mural nodule (arrow). **D.** The perfusion curve of this nodule steeply increases, even with less myometrium (curve number 3 in the figure), and then decreases in the later phases (type II curve, curve number 2 in the figure). DWI = diffusion-weighted imaging

Author Contributions

Conceptualization: Giacomo Avesani, Viviana La Manna. Data curation: Giacomo Avesani, Gianluca Caliolo, Viviana La Manna, Francesca Moro, Benedetta Gui, Federica Petta, Camilla Panico. Formal analysis: Giacomo Avesani, Gianluca Caliolo. Investigation: Giacomo Avesani, Gianluca Caliolo, Viviana La Manna, Francesca Moro, Benedetta Gui, Federica Petta, Camilla Panico. Methodology: Giacomo Avesani, Gianluca Caliolo, Riccardo Manfredi. Project administration: Giacomo Avesani, Benedetta Gui, Riccardo Manfredi. Resources: Giacomo Avesani, Francesca Moro, Antonia Carla Testa. Software: Giacomo Avesani, Gianluca

ORCID iDs

Giacomo Avesani
  https://orcid.org/0000-0001-9926-760X
Gianluca Caliolo
  https://orcid.org/0000-0002-5970-2440
Benedetta Gui
  https://orcid.org/0000-0002-5130-2100
Federica Petta
  https://orcid.org/0000-0001-7666-9278
Camilla Panico
  https://orcid.org/0000-0002-0472-1118
Viviana La Manna
  https://orcid.org/0000-0002-7880-2965
Francesca Moro
  https://orcid.org/0000-0002-5070-7245
Antonia Carla Testa
  https://orcid.org/0000-0003-2217-8726
Giovanni Scambia
  https://orcid.org/0000-0002-9503-9041
Riccardo Manfredi
  https://orcid.org/0000-0002-4972-9500

REFERENCES

1. Czernobilsky B, Borenstein R, Lancet M. Cystadenofibroma of the ovary. A clinicopathologic study of 34 cases and comparison with serous cystadenoma. *Cancer* 1974;34:1971-1981
2. Serov SF, Scully RE, Sobin LH. *Histological typing of ovarian tumours*. Geneva: World Health Organization, 1973
3. Outwater EK, Siegelman ES, Talerman A, Dunton C. Ovarian fibromas and cystadenofibromas: MRI features of the fibrous component. *J Magn Reson Imaging* 1997;7:465-471
4. Cho SM, Byun JY, Rha SE, Jung SE, Park GS, Kim BK, et al. CT and MRI findings of cystadenofibromas of the ovary. *Eur Radiol* 2004;14:798-804
5. Cho DH. Serous cystadenofibroma misdiagnosed as an ovarian malignancy. *BMJ Case Rep* 2018;11:e228223
6. Groutz A, Wolman I, Wolf Y, Luxman D, Sagi J, Jaffa AJ, et al. Cystadenofibroma of the ovary in young women. *Eur J Obstet Gynecol Reprod Biol* 1994;54:137-139
7. Jung DC, Kim SH, Kim SH. MR imaging findings of ovarian cystadenofibroma and cystadenocarcinofibroma: clues for the differential diagnosis. *Korean J Radiol* 2006;7:199-204
8. Shimizu S, Okano H, Ishitani K, Nomura H, Nishikawa T, Ohta H. Ovarian cystadenofibroma with solid nodular components masqueraded as ovarian cancer. *Arch Gynecol Obstet* 2009;279:709-711
9. Timmerman D, Testa AC, Bourne T, Ameye L, Jurkovic D, Van Holsbeke C, et al. Simple ultrasound-based rules for the diagnosis of ovarian cancer. *Ultrasound Obstet Gynecol* 2008;31:681-690
10. Patel-Lippmann KK, Sadowski EA, Robbins JB, Paroder V, Barroilhet L, Maddox E, et al. Comparison of international ovarian tumor analysis simple rules to society of radiologists in ultrasound guidelines for detection of malignancy in adnexal cysts. *AJR Am J Roentgenol* 2020;214:694-700
11. Nunes N, Ambler G, Foo X, Naftalin J, Widschwendter M, Jurkovic D. Use of IOTA simple rules for diagnosis of ovarian cancer: meta-analysis. *Ultrasound Obstet Gynecol* 2014;44:503-514
12. Garg S, Kaur A, Mohi JK, Sibia PK, Kaur N. Evaluation of IOTA simple ultrasound rules to distinguish benign and malignant ovarian tumours. *J Clin Diagn Res* 2017;11:TC06-TC09
13. Virgilio BA, De Blasis I, Sladkevicius P, Moro F, Zannoni GF, Arciuolo D, et al. Imaging in gynecological disease (16): clinical and ultrasound characteristics of serous cystadenofibromas in adnexa. *Ultrasound Obstet Gynecol* 2019;54:823-830
14. Jung SE, Lee JM, Rha SE, Byun JY, Jung JI, Hahn ST. CT and MR imaging of ovarian tumors with emphasis on differential diagnosis. *Radiographics* 2002;22:1305-1325
15. Takeuchi M, Matsuzaki K, Harada M. Ovarian adenofibromas and cystadenofibromas: magnetic resonance imaging findings including diffusion-weighted imaging. *Acta Radiol* 2013;54:231-236
16. Tang YZ, Liyanage S, Narayanan P, Sahdev A, Sohaib A, Singh N, et al. The MRI features of histologically proven ovarian cystadenofibromas-an assessment of the morphological and enhancement patterns. *Eur Radiol* 2013;23:48-56
17. Thomassin-Naggara I, Poncelet E, Jalaguier-Coudray A, Guerra A, Fournier LS, Stojanovic S, et al. Ovarian-Adnexal Reporting Data System Magnetic Resonance Imaging (O-RADS MRI) score for risk stratification of sonographically indeterminate adnexal masses. *JAMA Netw Open* 2020;3:e1919896
18. Takeuchi M, Matsuzaki K, Kusaka M, Shimazu H, Yoshida S, Nishitani H, et al. Ovarian cystadenofibromas: characteristic magnetic resonance findings with pathologic correlation. *J Comput Assist Tomogr* 2003;27:871-873
19. Byun JY. MR imaging findings of ovarian cystadenofibroma: clues for making the differential diagnosis from ovarian malignancy. *Korean J Radiol* 2006;7:153-155
20. McNulty JR. The ovarian serous cystadenofibroma; a report of 25 cases. *Am J Obstet Gynecol* 1959;77:1338-1344

21. Khashper A, Addley HC, Abourokbah N, Nougaret S, Sala E, Reinhold C. T2-hypointense adnexal lesions: an imaging algorithm. *Radiographics* 2012;32:1047-1064

22. Jeong YY, Outwater EK, Kang HK. Imaging evaluation of ovarian masses. *Radiographics* 2000;20:1445-1470

23. Moon WJ, Koh BH, Kim SK, Kim YS, Rhim HC, Cho OK, et al. Brenner tumor of the ovary: CT and MR findings. *J Comput Assist Tomogr* 2000;24:72-76

24. Joja I, Asakawa T, Mitsumori A, Nakagawa T, Hiraki Y, Kudo T, et al. Struma ovarii: appearance on MR images. *Abdom Imaging* 1998;23:652-656

25. Kim SH, Kim WH, Park KJ, Lee JK, Kim JS. CT and MR findings of Krukenberg tumors: comparison with primary ovarian tumors. *J Comput Assist Tomogr* 1996;20:393-398

26. Chung BM, Park SB, Lee JB, Park HJ, Kim YS, Oh YJ. Magnetic resonance imaging features of ovarian fibroma, fibrothecoma, and thecoma. *Abdom Imaging* 2015;40:1263-1272